International Journal of Natural Resources and Environmental Studies
ISSN: 3006-2012 (Print), ISSN: 3006-0834 (Online) | Volume 8, Number 3, Year 2026
DOI: https://doi.org/10.62051/ijnres.v8n3.21
Journal homepage: https://wepub.org/index.php/IJNRES/index

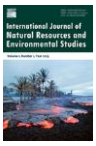

Electrocatalytic Nitrate Reduction for Selective Ammonia Production: Mechanisms and Prospects

Menghuai Tang*

College of Environmental Science and Engineering, Tongji University, Shanghai, China
*Corresponding Author: Menghuai Tang

ABSTRACT

Electrocatalytic nitrate reduction to ammonia driven by renewable energy offers the dual benefits of environmental remediation and sustainable ammonia synthesis. However, this process is a complex multi-electron, multi-proton reaction involving a variety of reaction pathways, making it crucial to understand its mechanism at the molecular level. This review first outlines the necessity and advantages of electrocatalytic nitrate reduction to ammonia, as well as its electrochemical principles and fundamentals. It then focuses on the reaction mechanisms and pathways, along with in situ characterization techniques used to monitor reaction intermediates and identify active sites. Finally, future research directions are proposed, and the applications and economic value in sustainable ammonia synthesis and energy conversion are systematically discussed. This review aims to decode the principles of nitrate reduction to ammonia and provide guidance for the rational design and development of electrocatalysts to achieve a sustainable and efficient nitrogen cycle.

KEYWORDS

Nitrate reduction; Electrocatalysis; Ammonia synthesis; Reaction mechanism.

1. INTRODUCTION

The nitrogen cycle (N cycle), as one of the most important biogeochemical cycles in global ecosystems, can generally be divided into three processes: nitrogen fixation, nitrification, and denitrification. Among these, the nitrification process (the oxidation of NH_3 to NO_2^- followed by oxidation to NO_3^-) and the denitrification process (the reduction of nitrate) are two central links in the global nitrogen cycle. However, disturbances from human activities such as excessive fertilization and the discharge of industrial wastewater and livestock wastewater have led to the excessive release of NO_3^-, causing an imbalance in the natural global nitrogen cycle. Therefore, artificially promoting the denitrification process is a key step in establishing a closed and stable N cycle [1]. So far, the main artificial methods for promoting denitrification include conventional biological, physical, and chemical treatments. However, the biological denitrification process suffers from problems such as strict microbial survival conditions, slow conversion rates, long retention times, complex operating conditions, and the generation of large amounts of sludge. Physical treatment processes, by contrast, focus on material displacement and concentration rather than elimination and conversion, and often require additional costs and processes for post-treatment. Chemical reduction treatment can selectively convert nitrate into harmless or high-value target products (such as N_2, NH_3), and this process can be driven by energy sources such as heat, light, and electricity. Among these, electrocatalytic nitrate reduction (NO_3RR) to ammonia can integrate environmental remediation with resource recovery, in line with the principles of the circular economy, and provides a transformative approach to addressing the global nitrogen cycle imbalance; this is also the focus of this review.

Due to its high stability and high solubility, NO_3^-can exist extensively, widely, and persistently in groundwater and surface water, while excessive NO_3^- can cause a series of ecological and environmental problems such as eutrophication and drinking water contamination [2, 3]. The quality of drinking water is directly related to human health, and excessive nitrate intake may lead to serious health problems. The World Health Organization and the U.S. Environmental Protection Agency have set the maximum contaminant levels (MCLs) for nitrate in drinking water at 50 ppm (NO_3^-) and 10 ppm (NO_3^---N), and the maximum contaminant level for nitrite at 0.03 ppm (NO_2^---N). Ammonia (NH_3) is one of the key chemicals in fields such as agriculture, chemical engineering, pharmaceuticals, and energy. At present, the annual production of ammonia reaches 175 million tons, with a value of about \$67 billion. According to statistics, approximately 80% of NH_3 is used for fertilizers, accounting for 40% of the agricultural fertilizer market [4]. At the same time, NH_3 has high practical value because of its high energy density, rich hydrogen content, high liquefaction temperature, and relatively low transportation and storage costs. However, artificial NH_3 synthesis currently still mainly relies on the energy- and carbon-emission-intensive Haber–Bosch process. Therefore, it is necessary to explore new green NH_3 synthesis technologies to alleviate the problems of high energy consumption and high emissions.

In summary, electrocatalytic nitrate reduction to ammonia (NO_3^--to-NH_3) driven by sustainable energy is regarded as one of the most promising frontier technologies for artificially promoting the denitrification process, as it can simultaneously achieve environmentally friendly treatment and the production of high-value-added chemicals. This technology offers multiple advantages: (1) it uses electrons as a green reducing agent, requires no additional additives, and causes no secondary pollution[5]; (2) it requires less space and involves a simpler process, and the electrocatalytic system can be seamlessly integrated into current water treatment processes[6]; (3) electrocatalytic nitrate reduction is highly efficient and can be carried out under relatively mild conditions at room temperature and atmospheric pressure[7, 8]; (4) The dissociation energy of the N=O bond is relatively low at 204 kJ mol^{-1}, and the high solubility of NO_3^- (>2 mol L^{-1}) gives NO_3^- excellent compatibility with liquid-phase electrocatalytic systems[9]; (5) it enables distributed and on-site/on-demand production of NH_3, which can also be further used to synthesize high-value nitrogen-containing products; (6) the electrical energy required for electrocatalytic reduction can be obtained from renewable clean energy, which not only enriches the modes of renewable energy storage and conversion but also enhances the capacity for green electricity consumption. Therefore, in view of these advantages, electrocatalytic nitrate reduction to ammonia (NO_3^--to-NH_3) provides an attractive and sustainable route for producing high-value ammonia and achieving wastewater denitrification while restoring the nitrogen cycle, and it can be used to construct the blueprint for a renewable and efficient ammonia production system as shown in Figure 1.

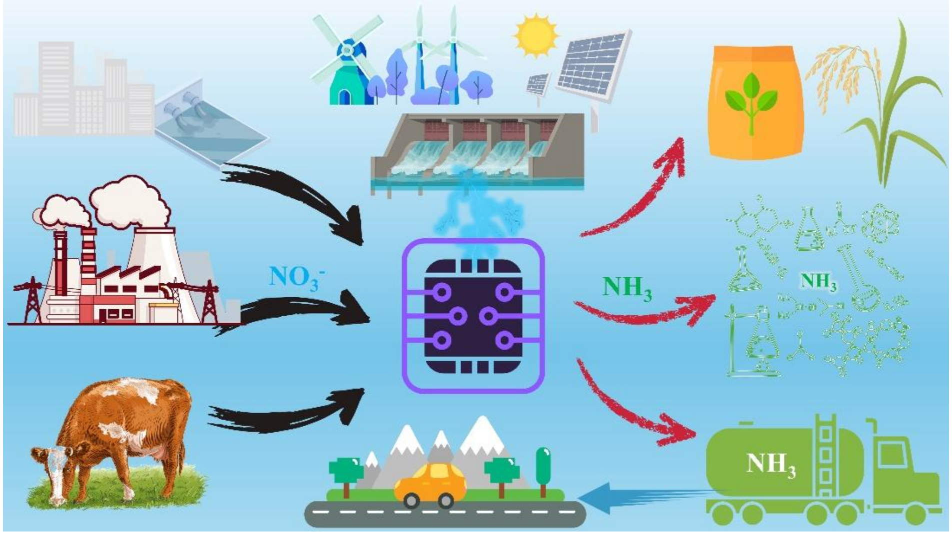

Figure 1. A conceptual cycle for synthesizing green NH_3 from NO_3^--containing wastewater

This review provides a comprehensive summary and evaluation of insights into the principles of the electrochemical NO_3^--to-NH_3 reduction process and concludes with prospects for future development trends and directions in this field. Specifically, insights into the electroreduction process are first introduced from two aspects: mechanistic discussion and mechanistic understanding, mainly focusing on the identification and recognition of reaction pathways, intermediates, and active species. Finally, the challenges facing the future development of NO_3RR are analyzed, and future research directions are proposed. We believe that this review will help advance the understanding of the electrocatalytic NO_3^--to-NH_3 process and provide inspiration for the future development of this field.

2. THE PRINCIPLE OF NO3RR

2.1. Mechanistic Discussion

2.1.1. Electrochemical Principles and Fundamentals

Each oxidation state of nitrogen is associated with a specific nitrogen species [10], and the standard equilibrium potential of nitrogen species is related to the solution pH. Under standard conditions, especially in highly alkaline reaction environments, N_2 and NH_3/NH_4^+ are the thermodynamically most stable nitrogen forms. Among them, because N_2 has the highest equilibrium potential (E0 = 1.246 V vs. SHE), N_2 is a more stable possible reduction product than NH_3 during the NO_3RR process [11]. Interestingly, although N_2 is theoretically the more likely reduction product, the reaction pathway can be influenced and the final product of NO_3RR can be further altered by changing certain parameters and selecting different catalysts. In recent years, the eight-electron process for the direct conversion of nitrate to NH_3 (Eq. 1) has attracted the interest of many researchers because of its economic and environmental value.

$$NO_3^- + 6H_2O + 8e^- \to NH_3 + 9OH^- \qquad E^0 = 0.69\, V\, vs. RHE. \tag{1}$$

In liquid-phase systems, the electrocatalytic reduction of nitrate, whether to form N_2 or ammonia, is a multi-proton-coupled multi-electron transfer process and requires a high activation energy barrier. This is because NO_3^- belongs to the D_3h point group and possesses a high-energy vacant antibonding π* orbital as its lowest unoccupied molecular orbital (LUMO). According to frontier orbital theory, when * NO_3^- reduction is initiated, electrons from the highest occupied state (HOS) of the electrocatalyst should be injected into the LUMO of NO_3^-. Therefore, the coupling between the valence orbitals of the catalyst active sites and the LUMO of NO_3^- directly affects the electron transfer between the electrocatalyst and NO_3^-, thereby determining the overpotential required for the initial potential of NO_3RR.

In summary, the reduction of nitrate to ammonia is a rather complex process, requiring the transfer of 8 electrons and 9 protons as well as a high activation energy barrier, which results in slow kinetics and low selectivity. Therefore, it is necessary to further understand the reaction pathways, the fundamental reactions during the process, and the intermediates involved, to improve the selectivity toward the target product.

2.1.2. Reaction Mechanism and Pathways

NO3RR involves multiple proton-coupled electron transfers and has various possible reaction pathways (as shown in Figure 2). During the reaction, various unstable intermediates are generated, such as $*NO_2^-$, $*NO$, and $*NH_2OH$, leading to a diverse product distribution, including N_2, NH_2OH, and NH_3[12]. In general, the reaction mechanism of NO_3RR can mainly be divided into two types: direct electrocatalytic reduction and indirect spontaneous electrocatalytic reduction. The specific mechanism is influenced by factors such as NO_3^- concentration, applied potential, catalyst type, and the pH of the electrolyte [13]. A comprehensive understanding of the reaction pathways is an important foundation for designing efficient electrocatalysts and advancing electrochemical reduction systems.

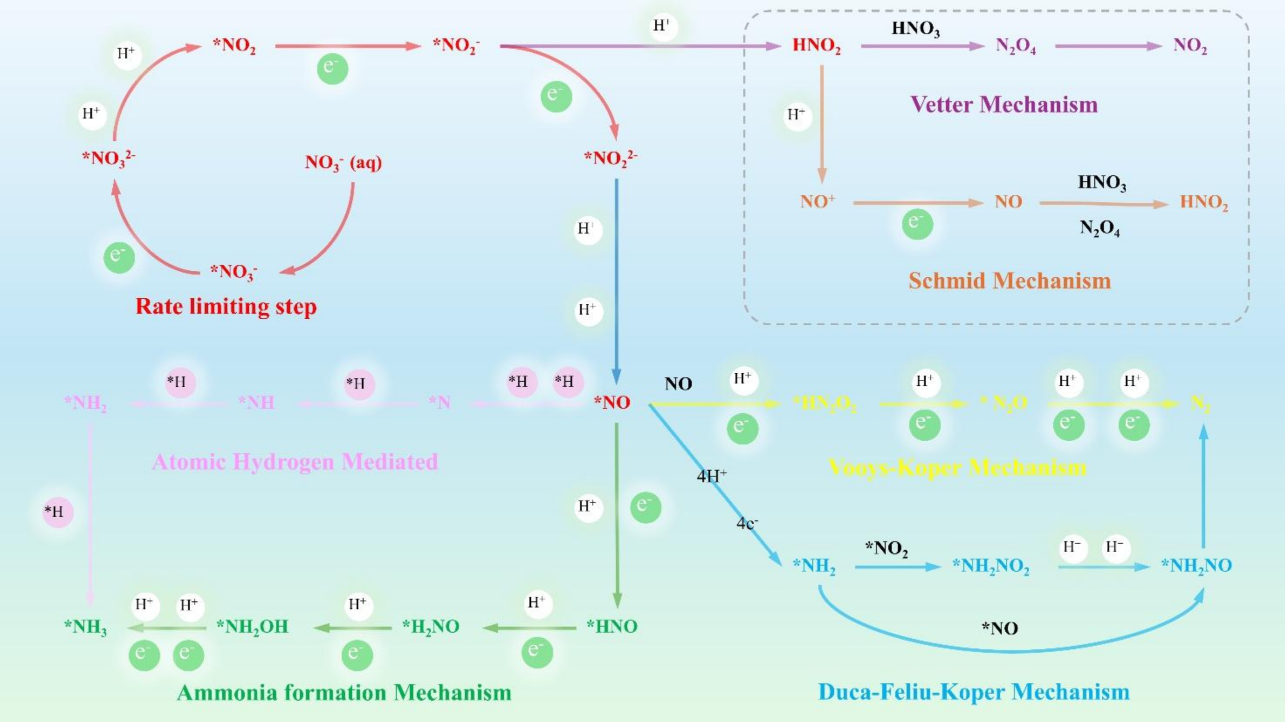

Figure 2. Schematic diagram of the electrochemical nitrate reduction mechanism.

2.1.2.1. Direct Electrocatalytic Reduction Mechanism

In most cases, nitrate reduction is carried out in a neutral or alkaline environment containing a low NO_3^- concentration and is therefore usually associated with the direct catalytic reduction mechanism [14]. The electrochemical reduction of nitrate involves reactant diffusion, adsorption, electron transfer, product desorption, and separation, among which the electron transfer of the electroactive species is key. In this mechanism, the electroactive species is nitrate, which directly participates in the electron transfer process [11]. Owing to factors such as differences in catalysts and applied potential, it can further be divided into two distinct pathways: cathodic electron-mediated reduction and adsorbed atomic hydrogen (*H)-mediated reduction.

(1) Cathodic electron-mediated reduction

This pathway is more likely to occur on electrode surfaces with a strong affinity for NO_3^- and a low affinity for *H [15]. Specifically, this pathway includes the rate-determining step of reducing nitrate to nitrite and the selectivity-determining step of further reducing nitrite, mainly involving the Duca-Felius-Koper mechanism, the Vooys-Koper mechanism, and the ammonia formation mechanism.

①Nitrate reduction to nitrite---the rate-determining step

At present, the conclusion accepted by most scholars is that the reduction of NO_3^- to NO_2^- is the rate-limiting step in the nitrate reduction reaction. This is because the energy of the lowest unoccupied molecular π* orbital (LUMO π*) of NO_3^- is very high, making it difficult for electrons to transfer into the π* orbital. This limits electron injections, so the transfer of the first electron during this conversion is often relatively difficult. Theaters such as the mass transport of NO_3^- in the electrolyte, its adsorption on the surface of the reaction electrode, and electron transfer during the reaction can all affect this rate-limiting step.

Before the first PCET step, NO_3^- ions must be adsorbed onto the active sites, so the mass transfer of NO_3^- in the electrolyte is particularly important. According to Fick's law, the NO_3^- concentration has a major influence on the diffusion and reduction rate of nitrate: when the NO_3^- concentration is low, the concentration gradient of NO_3^- ions near the electrode surface is small, and the mass-transfer diffusion process is slow. At this time, the co-adsorbed ions have a greater impact on the reaction rate, because other ions in the solution will inevitably be adsorbed onto the catalyst, which not only further slows the nitrate reduction rate but also leads to the occurrence of side reactions [11]. In contrast, when the $NO_3−$ concentration is high, the mass-transfer limitation of $NO_3−$ is weakened, and the factors that more strongly affect the reaction rate are the number of effective active sites on the catalyst surface and their activity [15].

The adsorption process of $NO_3−$at active sites usually occurs on the electrode surface (Eq. 2). Considering the molecular structure of $NO_3−$, it can generally be adsorbed onto the catalyst surface through two different bonding modes, namely by bonding to active sites on the electrode surface through either one or two O atoms. Theoretical calculations indicate that, compared with a single oxygen atom, bonding $NO_3−$to the catalyst surface through two oxygen atoms is the kinetically more favorable configuration [16, 17], while the configuration of the nitrate adsorbate depends on the combined effects of factors such as the electrode material, competing ions, solvent, and electrode potential.

The conversion of $*NO_3−$ to $*NO_2−$ driven by an externally applied potential specifically involves a three-step electrochemical–chemical–electrochemical (ECE) reaction. That is, a fundamental charge-transfer reaction of one electron occurs at each step: $*NO_3−$ is first converted into the short-lived $*NO_{32}$- through an electrochemical reaction (Eq. 3), and then $*NO_2$• is generated through a rapid radical hydrolysis reaction (Eq. 4). Finally, $*NO_2$• is reduced to $*NO_2−$ through a second charge-transfer reaction (Eq. 5). A portion of the generated $NO_2−$ may continue to adsorb on the surface, often maintaining a favorable oxygen-atom bidentate adsorption configuration, while another portion of $NO_2−$ may desorb and remain free in the electrolyte, which explains why the byproduct nitrite can always be detected in most NO_3RR processes [18].

$$NO_3^- + * \rightarrow * NO_3^-. \tag{2}$$

$$* NO_3^- + e^- \rightarrow * NO_3^{2-}. \tag{3}$$

$$* NO_3^{2-} + H_2O \rightarrow * NO_2 \bullet + 2OH^-. \tag{4}$$

$$* NO_2 \bullet + e^- \rightarrow * NO_2^-. \tag{5}$$

②Further reduction of nitrite --- the selectivity-determining step

$*NO_2−$ is one of the key metastable intermediates because it is one of the branching points leading to different reaction pathways and final products. Once $*NO_2−$ is formed, the non-desorbed nitrite intermediate ($*NO_2−$) is highly active on the electrocatalyst surface. Under certain conditions, $*NO_2−$ will further undergo electron transfer to form $*NO_{22}−$ (Eq. 6), and then further combine with protons and be hydrogenated to *NO (Eq. 7), which is another key intermediate in the NO_3RR process. The selective reduction of *NO will determine the subsequent reaction pathway and final products, which is of great significance for product selectivity. In fact, the choice of pathway mainly depends on the type of catalyst; meanwhile, one or more pathways may also coexist on the catalyst surface.

$$* NO_2^- + e^- \rightarrow * NO_2^{2-}. \tag{6}$$

$$* NO_2^{2-} + 2H^+ \rightarrow * NO + H_2O. \tag{7}$$

The subsequent reaction pathways following the selective reduction of *NO can be specifically divided into the following types:

Pathway I involves the direct reduction of *NO to *N (Eq. 8), followed by the combination of two *N species to form N_2 (Eq. 9) [19].

$$* NO + 2H^+ + 2e^- \rightarrow * N + H_2O. \tag{8}$$

$$* N + * N \rightarrow N_2. \tag{9}$$

Pathway II is the Vooys-Koper mechanism: a portion of *NO desorbs from the electrode surface and forms free NO in the aqueous phase, which then reacts with weaker adsorbed *NO to form the short-lived byproduct $*HN_2O_2$ (Eq. 10). Subsequently, a second proton-coupled electron transfer generates the $^*N_2O$ intermediate (Eq. 11). If the adsorption of $^*N_2O$ is weak, this favors the formation of N_2O. Conversely, once $^*N_2O$ is reduced on the catalyst surface rather than desorbing from the cathode surface, the adsorbed $^*N_2O$ is further reduced to $^*N_2O-$ (Eq. 12), which then attracts protons and electrons and readily form H_2O and N_2 (Eq. 13) [20, 21].

$$* NO + NO + e^- + H^+ \rightarrow * HN_2O_2. \tag{10}$$

$$* HN_2O_2 + e^- + H^+ \rightarrow * N_2O + H_2O. \tag{11}$$

$$* N_2O + e^- \rightarrow * N_2O^-. \tag{12}$$

$$* N_2O^- + e^- + 2H^+ \rightarrow N_2 + H_2O. \tag{13}$$

Pathway III is the Duca-Feliu-Koper mechanism, which is mainly active under alkaline conditions. Within an appropriate potential range, $^*NO$ can be directly reduced to $^*NH_2$ via electron transfer (Eq. 14) [22]. Then, the $^*NO$ species reacts with $^*NH_2$ through Langmuir-Hinshelwood recombination (Eq. 15), forming the intermediate N-nitrosamine (NH_2NO), a transient species that can decompose into N_2 (Eq. 16) [19, 23].

$$* NO + 4e^- + 4H^+ \rightarrow * NH_2 + H_2O. \tag{14}$$

$$* NO + * NH_2 \rightarrow * NH_2NO. \tag{15}$$

$$* NH_2NO \rightarrow N_2 + H_2O. \tag{16}$$

Pathway IV involves the electron reduction of $^*NO$ to form $^*HNO$ (Eq. 17). $^*HNO$ rapidly dimerizes to generate the intermediate hyponitrous acid ($^*H_2N_2O_2$) (Eq. 18), which is a stable intermediate under appropriate acidic conditions, whereas its monoanionic form ($^*HN_2O_2-$) is unstable and readily decomposes to produce $^*N_2O$ (Eq. 19) [24].

$$* NO + H^+ + e^- \rightarrow * HNO. \tag{17}$$

$$* HNO + * HNO \rightarrow * H_2N_2O_2. \tag{18}$$

$$* H_2N_2O_2 \rightarrow * N_2O + H_2O. \tag{19}$$

Pathway V is the ammonia formation mechanism and is the desired process. This is a continuous charge-transfer pathway, in which a typical process is that when the intermediate $^*NO$ is reduced by one electron, $^*HNO$ is first formed (Eq. 20), then it continues to gain one electron to form $^*H_2NO$ (Eq. 21), and is subsequently reduced to hydroxylamine ($^*NH_2OH$) (Eq. 22). Notably, the $^*NH_2OH$ intermediate readily desorbs from the catalyst surface, forming the hydroxylamine byproduct. Finally, the adsorbed hydroxylamine continues to be reduced to form ammonia (Eqs. 23-25).

$$* NO + e^- + H^+ \rightarrow * HNO. \tag{20}$$

$$* HNO + e^- + H^+ \rightarrow * H_2NO. \tag{21}$$

$$* H_2NO + e^- + H^+ \rightarrow * NH_2OH. \tag{22}$$

$$* NH_2OH + 2e^- + 2H^+ \rightarrow * NH_3 + H_2O. \tag{23}$$

$$* NH_3 \rightarrow NH_3 + *. \tag{24}$$

$$NH_3 + H^+ \rightarrow NH_4^+. \tag{25}$$

In addition, Katsounaros et al. found that $^*NH_2OH$ can be consumed by several chemical reactions and further converted into N_2 (Eq. 26) or N_2O (Eq. 27) [19].

$$* NH_2OH + HNO \rightarrow N_2 + H_2O. \tag{26}$$

$$* NH_2OH + HNO_2 \rightarrow N_2O + H_2O. \tag{27}$$

It is worth noting that the adsorption configuration of $^*NO$ determines the different reaction pathways and the corresponding electrocatalytic selectivity toward the products N_2 or NH_3[11]. There are three geometric configurations for *NO adsorption: O-end adsorption, N-end adsorption, and side-on NO adsorption. Side-on NO adsorption can be further subdivided into oxygen-side hydrogenation and nitrogen-side hydrogenation according to the hydrogenation site [25]. In the mechanism of ammonia formation, the various adsorption configurations of NO can all be converted into the final product NH_3 through different pathways. This transformation follows an electrochemical-electrochemical (EE) mechanism, and the typical pathways are discussed below.

For configuration I, adsorption occurs via the O end, so the nitrogen atom is preferentially attacked by protons and electrons, thereby first promoting the formation of *ONH (Eq. 28). The subsequent reaction pathway for further ammonia generation includes two direct protonation reactions at the nitrogen atom: *ONH needs to gain one electron to produce $*ONH_2$ (Eq. 29), and rapid charge transfer drives the reduction of $*ONH_2$ to NH_3, leaving behind *O species (Eq. 30) [26]. Subsequently, the remaining *O is further reduced by two protons to a water molecule in an electrochemical step (Eq. 31). Among these electrochemical steps, the protonation of *ON to *ONH is the rate-determining step [27].

$$* ON + e^- + H^+ \rightarrow * ONH. \tag{28}$$

$$* ONH + e^- + H^+ \rightarrow * ONH_2. \tag{29}$$

$$* ONH_2 + e^- + H^+ \rightarrow NH_3 + * O. \tag{30}$$

$$* O + 2e^- + 2H^+ \rightarrow H_2O. \tag{31}$$

Configuration II involves N-end adsorption, and the subsequent steps are related to the N–N bond interaction between *NO and its solvated counterpart NO(aq). When an N–N bond is formed between *NO and NO (aq), the intermediate proton and electron are attracted, following the Vooys–Koper mechanism introduced above [28]. When no N–N bond is formed between *NO and NO(aq), *NO is first reduced to *NOH through proton-coupled electron transfer (Eq. 32), which is the key species for NH3 formation. Then, further protonation occurs at the oxygen atom, leading to the formation of *N and H_2O molecules (Eq. 33). Subsequently, *N ultimately forms NH_3 through three consecutive proton-coupled electron transfer steps (Eqs. 34–36) [29].

$$* NO + e^- + H^+ \rightarrow * NOH. \tag{32}$$

$$* NOH + e^- + H^+ \rightarrow * N + H_2O. \tag{33}$$

$$* N + e^- + H^+ \rightarrow * NH. \tag{34}$$

$$* NH + e^- + H^+ \rightarrow * NH_2. \tag{35}$$

$$* NH_2 + e^- + H^+ \rightarrow * + NH_3. \tag{36}$$

Configuration III involves side-on adsorption of NO, i.e., parallel adsorption. In this case, the protonation site (the N side or the O side) plays a decisive role in the subsequent PCET steps and the corresponding products [30]. When protonation occurs at the nitrogen atom, the intermediate *HNO is first formed, and the subsequent reduction steps follow a reaction pathway like that for O-end adsorption. In contrast, when protonation occurs at the oxygen atom, the intermediate *NOH is first formed (Eq. 37). Notably, further protonation at either the oxygen or nitrogen atom can generate *N or *NHOH. When OH is removed from the *NOH intermediate to obtain *N, NH_3 is subsequently produced through a pathway like that of N-end adsorption. When *NHOH is formed (Eq. 38), further protonation leads to $*NH_2OH$ (Eq. 39), which is achieved through two PCET processes at the nitrogen atom of *NOH. Finally, H_2O is released (Eq. 40), and $*NH_2$ is then hydrogenated to NH_3 through a rapid electrochemical reduction process (Eq. 41).

$$* NO + e^- + H^+ \rightarrow * NOH. \tag{37}$$

$$* NOH + e^- + H^+ \rightarrow * NHOH. \tag{38}$$

$$* NHOH + e^- + H^+ \rightarrow * NH_2OH. \tag{39}$$

$$*NH_2OH + e^- + H^+ \rightarrow *NH_2 + H_2O. \quad (40)$$

$$*NH_2 + e^- + H^+ \rightarrow * + NH_3. \quad (41)$$

(2) Adsorbed Atomic Hydrogen (*H)-Mediated Reduction

Adsorbed atomic hydrogen-mediated reduction of nitrate usually occurs at low overpotentials, and noble metals have a high affinity for hydrogen; therefore, the surfaces of noble metal catalysts are also more prone to undergo adsorbed atomic hydrogen-mediated reduction. In the process of adsorbed atomic hydrogen-mediated reduction, the initial stage involves the generation of *H, namely the first step in the HER process (the Volmer step) [31]. HER follows two key mechanisms: Volmer-Tafel [32] and Volmer-Heyrovsky [33]. In the Volmer step, H_2O molecules/protons adsorbed on the electrode surface capture electrons to generate *H (Eqs. 42, 43). The Tafel step involves the recombination of two *H species to produce molecular hydrogen (H_2) (Eq. 44), whereas the Heyrovsky step combines one *H with one proton and one electron to form H_2 (Eq. 45).

$$*H_2O + e^- \rightarrow *H + OH^-. \quad (42)$$

$$*H_3O^+ + e^- \rightarrow *H + H_2O. \quad (43)$$

$$*H + *H \rightarrow H_2. \quad (44)$$

$$*H + H_3O^+ + e^- \rightarrow H_2 + H_2O. \quad (45)$$

Active hydrogen (*H), as a key intermediate for subsequent hydrogenation in NO_3RR, possesses strong reducing power (E0(H+/H) = −2.31 V vs. RHE) [34] and can gradually reduce adsorbed high-valence nitrate into intermediates with various valence states. The deoxygenation steps proceed along the pathway of $*NO_3-$、 $*NO_2-$, and *NO (Eqs. 46–49), among which the reaction between atomic *H and $*NO_3-$ is considered the rate-determining step in the atomic *H (ads)-mediated NO_3RR process[35]. Like electron-mediated reduction, different hydrogenation behaviors on *NO intermediate can also lead to changes in the reaction pathway, and the hydrogenation behaviors are classified as terminal hydrogenation and alternating hydrogenation [36].

$$*NO_3^- + *H \rightarrow *HNO_3^- + H_2O. \quad (46)$$

$$*HNO_3^- + *H \rightarrow *NO_2^- + H_2O. \quad (47)$$

$$*NO_2^- + *H \rightarrow *HNO_2^-. \quad (48)$$

$$*HNO_2^- + *H \rightarrow *NO + OH^-. \quad (49)$$

When the *NO intermediate undergoes terminal N hydrogenation [37], *H interacts with the N atom to form *HNO (Eq. 50), which is then stepwise hydrogenated to ultimately generate the target product NH_3 (Eqs. 51, 52). The remaining *O will be reduced to H_2O molecules in the subsequent electrochemical process (Eq. 53).

$$*NO + *H \rightarrow *HNO. \quad (50)$$

$$*HNO + *H \rightarrow *H_2NO. \quad (51)$$

$$*H_2NO + *H \rightarrow NH_3 + *O. \quad (52)$$

$$*O + 2*H \rightarrow H_2O. \quad (53)$$

When the *NO intermediate undergoes terminal O hydrogenation [38], *H attacks the O atom, thereby forming *NOH (Eq. 54). Then, *H continues to react with the O atom, reducing *NOH to *N and an H_2O molecule (Eq. 55). Subsequently, *N undergoes successive hydrogenation steps to form the final product NH3 (Eqs. 56–58).

$$*NO + *H \rightarrow *NOH. \quad (54)$$

$$*NOH + *H \rightarrow *N + H_2O. \quad (55)$$

$$*N+*H\rightarrow*NH. \tag{56}$$

$$*NH+*H\rightarrow*NH_2. \tag{57}$$

$$*NH_2+*H\rightarrow*+NH_3. \tag{58}$$

It is worth noting that the reaction site during the hydrogenation process may undergo switching, that is, it may shift between the N atom and the O atom. For example, it has been reported [39] that after *NO is hydrogenated at the O end to form *NOH (Eq. 59), the subsequent hydrogenation step may transfer to the N end, further converting *NOH into *NHOH (Eq. 60) rather than *N. Subsequently, *NHOH is reduced to hydroxylamine ($*NH_2OH$) (Eq. 61), followed by continuous electrochemical conversion that ultimately yields NH3 (Eq. 62).

$$*NO+*H\rightarrow*NOH. \tag{59}$$

$$*NOH+*H\rightarrow*NHOH. \tag{60}$$

$$*NHOH+*H\rightarrow*NH_2OH. \tag{61}$$

$$*NH_2OH+2*H\rightarrow*+NH_3+H_2O. \tag{62}$$

When atomic hydrogen-mediated reduction proceeds along the pathway of $*NO_3^-$、$*NO_2^-$、*NO、*N、*NH, and $*NH_2$. It is well known that the *N generated during this process can dimerize to form N_2, while NH_3 dominates among the final products because the migration energy barrier of *N (0.75 eV) is higher than that of *H (0.10 eV), and the formation of N-H bonds is energetically more favorable than the formation of N-N bonds[40]. This also indicates that during the electrochemical NO_3RR process, H_2 (the HER side reaction) is more likely to occur as a byproduct than N_2. These competing side-reaction pathways significantly affect the efficiency of NO_3RR, and suppressing the HER side reaction plays an important role in improving NH_3 selectivity. However, in the consecutive hydrogenation steps leading to NH_3 formation, active *H plays a crucial role. An insufficient supply of *H slows the rate of NH_3 formation, whereas an excessive supply leads to overaccumulation of *H, increasing the likelihood of *H dimerization and favoring HER rather than nitrate reduction [41]. In summary, *H plays a dual role in the NO_3RR process; therefore, a delicate balance must be achieved between insufficient and excessive *H supply, so that the rates of *H supply and consumption are kinetically matched. This is essential for optimizing the reaction pathway and improving the Faradaic efficiency (FE) of NO_3RR .For example, Yang et al. [42]exploited the strong water-splitting capability of nickel phosphide (Ni_2P), which possesses high conductivity and a Pt-like electronic structure, enabling it to provide abundant *H during the NO_3RR process (a high *H supply rate). By introducing low-valent iron species, NO_3^- can be spontaneously reduced to NO_2^-, while the low-valent iron is simultaneously converted into Fe_2O_3, thereby accelerating the overall reduction rate (increasing the *H consumption rate). At the same time, the generated Fe_2O_3 can consume excess *H and be promptly reduced back to low-valent iron species, thus kinetically matching the rates of *H supply and consumption. As a result, its FE can exceed 90% over a wide potential range of 0.3–0.9 V; the maximum NH_3 yield can reach as high as 120.1 mg h-1cm^{-2}; and it also delivers excellent performance over a wide NO_3^- concentration window and at a prolonged industrial current density of 1000 mA cm^{-2}.

2.1.2.2. Indirect autocatalytic electroreduction mechanism

The indirect autocatalytic mechanism occurs only in highly acidic media containing nitrite (>10-6 M) and high concentrations of nitrate (1.0–4.0 M) [43]. In the indirect autocatalytic reduction mechanism, NO_3^- does not constitute the true electroactive species and does not directly participate in the electron transfer process [30]. Instead, the intermediate products NO+ or NO_2 generated by nitrate reduction act as the true electroactive species to trigger this autocatalytic cycle. In the autocatalytic reaction, an increase in the concentration of the intermediate electroactive species leads to a rapid increase in the reaction rate. In the indirect electrocatalytic reduction of nitrate, only a very small overpotential is required, and the process is mainly selective toward HNO_2/NO+ and NO_2[44]. Depending on whether the electroactive species is the reaction intermediate NO_2 or NO+, the autocatalytic reduction process can be divided into two different pathways: the Vetter process and the Schmid process [30, 45].

Vetter considered this mechanism to be heterogeneous, with the electroactive species being NO_2, which is formed on the electrode surface based on a preceding slow heterogeneous chemical reaction. In the Vetter process, the focus is on the generation of NO_2, which is then reduced to NO_2- (Eq. 63) and subsequently protonated to HNO_2 in a highly acidic environment (Eq. 64), representing an acid-base equilibrium under acidic conditions. Thereafter, HNO_2 reacts with HNO_3 to produce unstable N_2O_4 (Eq. 65), which rapidly decomposes into two NO_2 molecules (Eq. 66), thereby regenerating the electroactive species NO_2. It is worth noting that although two NO_2 species are produced, only one enters the autocatalytic cycle, leading to an increase in the concentration of the intermediate electroactive species and accelerating the rate of nitrate reduction.

$$NO_2 + e^- \rightarrow NO_2^-. \tag{63}$$

$$NO_2^- + H^+ \rightarrow HNO_2 \quad pK_a = 3.4. \tag{64}$$

$$HNO_2 + HNO_3 \rightarrow N_2O_4 + H_2O. \tag{65}$$

$$N_2O_4 \rightarrow 2NO_2. \tag{66}$$

In contrast, Schmid and co-workers considered this reaction mechanism to be homogeneous, in which the electroactive species NO^+ (also regarded as HNO_2) is obtained from the protonation of nitrite formed in the layer near the electrode under strongly acidic conditions. In the Schmid mechanism, HNO_2 is first protonated and decomposed in a highly acidic environment to generate NO^+ (Eq. 67), which then captures an electron and is reduced to the intermediate NO (Eq. 68). The final product HNO_2 can be formed either through the reaction of two NO species with N_2O_4 in an aqueous medium (Eq. 69) or directly through the reaction of NO with nitric acid (Eq. 70), although some scholars believe that the latter reaction proceeds preferentially [46]. Similarly, because the amount of HNO_2 generated in this mechanism exceeds the amount consumed, this likewise leads to an increase in the concentration of the intermediate electroactive species, thereby accelerating the rate of nitrate reduction.

$$HNO_2 + H^+ \rightarrow NO^+ + H_2O \quad pK_a = 3.29. \tag{67}$$

$$NO^+ + e^- \rightarrow NO. \tag{68}$$

$$2NO + N_2O_4 + H_2O \rightarrow 4HNO_2. \tag{69}$$

$$2NO + HNO_3 + H_2O \rightarrow 3HNO_2. \tag{70}$$

It should be noted that once the nitric acid concentration exceeds 4.0 M, reactions (71) and (72) replace the original reactions, regenerating NO and N_2O_4. Since this conversion process does not involve electrochemical charge transfer, it is not included in the autocatalytic cycle of indirect electrocatalytic NO_3- reduction.

$$4HNO_3 \rightarrow 4NO + 3O_2 + 2H_2O. \tag{71}$$

$$4HNO_3 \rightarrow 2N_2O_4 + O_2 + 2H_2O. \tag{72}$$

2.2. Mechanistic Insights (In Situ Characterization)

2.2.1. Monitoring of Reaction Intermediates

During the NO_3RR process, probing changes at the electrode–electrolyte interface and understanding the transformation pathways of intermediates are crucial for identifying the reaction microenvironment and gaining an in-depth understanding of the mechanism. However, because most intermediates are unstable during the reaction, and their generation and consumption rates are matched and rapid, their lifetimes are extremely short, posing challenges for their identification and characterization. Therefore, electrochemical in situ characterization under real-time reaction conditions helps reveal the transient intermediates of reactants and the dynamic structure of catalysts, thereby enabling analysis of the nitrate reduction mechanism.

2.2.1.1. In situ differential electrochemical mass spectrometry (DEMS)

This technique is often used for the in-situ detection of volatile intermediates/products and their structural characteristics during electrochemical reactions, and this test is more sensitive to reaction conditions (such as reaction potential and reaction time). Yang et al. [42] detected mass-to-charge ratio signals of 46, 30, 31, 32, and 17, corresponding to NO_2, NO, HNO, NHOH, and NH_3, respectively. The authors preliminarily inferred that the subsequent reaction pathway of Fe-Ni_2P from $*NO_2$ to $*NH_3$ is $*NO_2 \rightarrow *NO \rightarrow *HNO \rightarrow *NHOH \rightarrow *NH \rightarrow *NH_2 \rightarrow *NH_3$.

2.2.1.2. Electrochemical in situ infrared spectroscopy (in situ IR)

This technique is often used to monitor in real time changes in the chemical bonds of adsorbed intermediates on the catalyst surface, and in the spectra, the positive and negative bands correspond to the formation and consumption of reactive intermediates, respectively. Chen et al. [47] used in situ attenuated total reflection infrared absorption spectroscopy to capture intermediates adsorbed on the electrode during NO_3RR. As the potential increased, the peak intensity of the characteristic band at 1215 cm^{-1} gradually increased, indicating the continuous consumption of NO_3- species during electrolysis. In addition, the peak at 1628 cm^{-1} can be attributed to the hydrogenated intermediate $*NH^2$. The peak at 1721 cm-1 gradually intensified with increasing potential, indicating the presence of $*NH_3$ species.

2.2.1.3. Electrochemical in situ electron spin resonance (ESR)

This technique is commonly used to identify active hydrogen, because active hydrogen is a key hydrogenation intermediate in the nitrate reduction reaction. This finding has changed the traditional catalyst design principle focused on suppressing water dissociation and has opened a new pathway for the development of highly efficient catalysts. Lv et al. [48] used electron paramagnetic resonance (EPR) spectroscopy to monitor the *H species generated on the catalyst surface, using 5,5-dimethyl-1-pyrroline-N-oxide (DMPO) as the *H trapping agent. In the presence of nitrate, the intensity of the DMPO-H spectrum was significantly lower than in the absence of nitrate, indicating that the reduction of NO_3- on the Ni-MoS_2 catalyst consumes *H. Taking advantage of the ability of tert-butanol (t-BuOH) to capture *H, its performance before and after introduction was compared, and it was found that the performance of NO_3RR was weakened, further confirming the importance of *H species and that nitrate reduction consumes *H.

2.2.1.4. In situ Raman spectroscopy

Raman spectroscopy probes molecular vibrations through the inelastic scattering of lasers in the near-infrared, visible, or near-ultraviolet range. This technique inherently reduces interference from water, which is a major advantage for aqueous electrolyte systems, and it is particularly effective for detecting nonpolar species. By taking advantage of these intrinsic benefits, in situ Raman spectroscopy can generally provide information in two aspects. On the one hand, it can directly detect reactants and intermediates during the NO_3RR process. On the other hand, Raman spectroscopy is often used to reveal changes in metal valence states (as introduced in the section on active-site identification). To further clarify the changes in intermediate products during the NO_3RR process, Lu et al. [49] conducted in situ Raman spectroscopy analysis. The Raman bands centered at 982 and 1045 cm^{-1} are associated with the vibrational modes of SO_4^{2}- and NO_3- in the electrolyte, respectively. As NO_3RR proceeds, the peak intensities corresponding to adsorbed * NO_3- (1370 cm^{-1}) and produced NH_3 (1140 cm^{-1}) gradually increase. This indicates that NO_3- is gradually adsorbed on the catalyst surface and further reduced to generate NH_3, while part of it desorbs into the solution. Meanwhile, the Raman bands at 1510, 1540, and 1610 cm^{-1} represent the *NH, *NOH, and $*NH_3$ intermediate species, respectively, and their signals increase significantly with reaction time. This further indicates the formation of the corresponding intermediates and provides evidence for understanding and confirming the reduction mechanism.

2.2.2. Identification of Active Sites

During the NO_3RR process, the adsorption of multiple intermediates and extensive electron transfer can occur, which may alter the state and structure of the catalyst [50]. Determining the active species under electrocatalytic reaction conditions is crucial for designing efficient electrocatalysts, and excellent performance can be achieved by rationally constructing active components for nitrate reduction. However, some changes during the NO_3RR process are unstable or reversible, making them difficult to measure through ex situ experiments. Therefore, electrochemical in situ characterization for revealing the dynamic structure (phase transitions) and valence-state evolution (changes in the coordination environment) of catalytic materials is indispensable.

2.2.2.1. Electrochemical in situ X-ray absorption spectroscopy (XAS)

Electrochemical in situ XAS testing is an advanced method for identifying the active components of catalysts under electrochemical reaction conditions. It is widely used to study changes in the oxidation states of metal atoms within catalysts during the reaction process. Zhang et al. [51] used in situ XAFS to monitor the structural changes of Cu_3N/GDY during electrolysis. During the reaction, the adsorption edge energy of Cu_3N/GDY gradually decreased from 8981 eV to 8980 eV, and after the reaction ended, the adsorption edge energy returned to 8981 eV, indicating that Cu_3N was reduced during the NO_3RR process, with the oxidation state of copper changing from +1 to approximately 0, and then recovering to +1 after the voltage was removed. The in-situ EXAFS spectra also showed that the Cu-N bond in Cu_3N/GDY decreased significantly at a voltage of -0.9 V vs. RHE and recovered after the voltage was removed. Based on the above analysis, under the high reduction potential of -0.9 V vs. RHE, the continuously generated individual Cu^0 sites in the catalyst are true active sites for NO3RR.

2.2.2.2. In situ Raman spectroscopy

Raman spectroscopy is often used to reveal changes in metal valence states and is usually conducted using both a Raman spectrometer and an electrochemical workstation. Yang et al. [42] used Raman spectroscopy to observe changes in the Fe-Ni_2P catalyst during the reaction process. The spectra showed that, after contact with an electrolyte containing NO_3- without any applied potential, a characteristic Raman peak closely associated with Fe-O bond vibrations appeared at 685 cm^{-1}. However, when the nitrate supply was stopped and electrochemical reduction was carried out at -0.6 V vs. RHE for 20 minutes, this Raman peak disappeared. Investigation of the effect of potential revealed that, as the applied potential decreased, the characteristic Fe-O peak disappeared below -0.5 V vs. RHE. Moreover, when the electrolyte contained only KOH, the characteristic Fe-O Raman peak also disappeared. These results indicate that low-valent Fe species undergo spontaneous redox reactions with NO_3- to form Fe_2O_3 species, which are then electrochemically reduced in situ to Fe at potentials of -0.5 V vs. RHE and below, enabling a sustained long-term dynamic iron valence cycling process.

3. SUMMARY AND OUTLOOK

Electrochemical nitrate reduction (NO_3RR) is regarded as a highly promising method for ammonia synthesis. Driven by renewable energy, it avoids the high-pressure and high-temperature conditions required by the conventional Haber-Bosch ammonia synthesis process, thereby significantly reducing carbon emissions and energy consumption. Although this technology has made remarkable progress, many challenges and opportunities remain in the application of NO_3RR for ammonia production. Future research should focus on the following key directions:

3.1. A Unified Evaluation System

Although the electrocatalysis field has strongly called for the establishment of standardized testing and evaluation criteria, many existing studies still fail to provide intuitive and comparable assessments of catalyst quality. Without uniform testing conditions, the performance of different catalysts cannot be compared reliably. A high ammonia yield alone is insufficient to evaluate catalyst effectiveness; factors such as electrolyte concentration, pH, and potential selection must also be considered, along with their impact on energy consumption.

3.2. Practical Applications

At present, most studies on NO_3RR are conducted using synthetic solutions, overlooking the challenges associated with practical applications in complex wastewater matrices. From a practical perspective, it is crucial to evaluate nano catalysts using real nitrate-containing wastewater samples (such as those containing Ca^{2+}、 Mg^{2+}, and organic matter), because this will provide more accurate insights into the long-term stability of the catalysts and the efficiency of ammonia collection. In addition, attention should be paid to the design and fabrication of electrochemical devices for the industrialization of NO_3RR under real wastewater conditions.

3.3. Economic Value

Although NO_3RR is usually a cathodic process, the corresponding oxidation reactions of anodic molecules can also be utilized. Thus, by coupling NO_3RR with other anodic reactions, energy consumption can be reduced, and high-value byproducts can be generated. At the same time, attention should be paid to the potential for recovering high-value byproducts; for example, electrolytes containing elements such as nitrogen (N), phosphorus (P), and potassium (K) can also be recovered as fertilizers, thereby increasing the added value of the process.

3.4. AI-Assisted Rational Catalyst Design

Future catalyst development will increasingly rely on the “intelligent design” paradigm. From the perspective of theoretical simulation, advanced computational technologies such as density functional theory and artificial intelligence should be employed to guide the prediction and screening of high-performance catalysts. This approach will also help optimize reactor operating parameters, predict catalytic enhancement mechanisms, and guide the rational design of reaction systems, thereby promoting a paradigm shift from “trial and error” to “rational design.”

CONFLICTS OF INTEREST

The authors declare that they have no conflict of interest.

REFERENCES

[1] N. Gruber, J.N. Galloway, An Earth-system perspective of the global nitrogen cycle, Nature 451(7176) (2008) 293–296.

[2] V. Rosca, M. Duca, M.T. de Groot, M.T.M. Koper, Nitrogen Cycle Electrocatalysis, Chemical Reviews 109(6) (2009) 2209–2244.

[3] J. Penuelas, J. Sardans, Human-driven global nutrient imbalances increase risks to health, Eco-Environment & Health 2(4) (2023) 246–251.

[4] H.-j. Chen, Z.-q. Xu, S. Sun, Y. Luo, Q. Liu, M.S. Hamdy, Z.-s. Feng, X. Sun, Y. Wang, H.-j. Chen, Plasma-etched Ti2O3 with oxygen vacancies for enhanced NH3 electrosynthesis and Zn–NO3− batteries Plasma-etched Ti2O3with oxygen vacancies for enhanced NH3 electrosynthesis and Zn–NO3− batteries, Inorganic Chemistry Frontiers 9(18) (2022) 4608–4613.

[5] C. Zhang, Y. Zhang, R. Deng, L. Yuan, Y. Zou, T. Bao, X. Zhang, G. Wei, C. Yu, C. Liu, Enabling Logistics Automation in Nanofactory: Cobalt Phosphide Embedded Metal–Organic Frameworks for Efficient Electrocatalytic Nitrate Reduction to Ammonia, Advanced Materials 36(26) (2024).

[6] Y. Chen, S. Ji, C. Chen, Q. Peng, D. Wang, Y. Li, Single-Atom Catalysts: Synthetic Strategies and Electrochemical Applications, Joule 2(7) (2018) 1242–1264.

[7] S. Ye, Z. Chen, G. Zhang, W. Chen, C. Peng, X. Yang, L. Zheng, Y. Li, X. Ren, H. Cao, D. Xue, J. Qiu, Q. Zhang, J. Liu, S. Ye, Elucidating the activity, mechanism and application of selective electrosynthesis of ammonia from nitrate on cobalt phosphide, Energy & Environmental Science 15(2) (2022) 760–770.

[8] P. Xu, S. Agarwal, L. Lefferts, Mechanism of nitrite hydrogenation over Pd/γ-Al2O3 according a rigorous kinetic study, Journal of Catalysis 383 (2020) 124–134.

[9] W.-J. Sun, H.-Q. Ji, L.-X. Li, H.-Y. Zhang, Z.-K. Wang, J.-H. He, J.-M. Lu, Built-in Electric Field Triggered Interfacial Accumulation Effect for Efficient Nitrate Removal at Ultra-Low Concentration and Electroreduction to Ammonia Built-in Electric Field Triggered Interfacial Accumulation Effect for Efficient Nitrate Removal at Ultra-Low Concentration and Electroreduction to Ammonia, Angewandte Chemie International Edition 60(42) (2021) 22933–22939.

[10] J. Yuan, H. Yin, X. Jin, D. Zhao, Y. Liu, A. Du, X. Liu, A.P. O'Mullane, A practical FeP nanoarrays electrocatalyst for efficient catalytic reduction of nitrite ions in wastewater to ammonia, Applied Catalysis B: Environmental 325 (2023) 122353.

[11] H. Xu, Y. Ma, J. Chen, W.-x. Zhang, J. Yang, H. Xu, Electrocatalytic reduction of nitrate – a step towards a sustainable nitrogen cycle, Chemical Society Reviews 51(7) (2022) 2710–2758.

[12] G.-F. Chen, Y. Yuan, H. Jiang, S.-Y. Ren, L.-X. Ding, L. Ma, T. Wu, J. Lu, H. Wang, Electrochemical reduction of nitrate to ammonia via direct eight-electron transfer using a copper–molecular solid catalyst, Nature Energy 5(8) (2020) 605–613.

[13] Y. Wang, C. Wang, M. Li, Y. Yu, B. Zhang, Y. Wang, Nitrate electroreduction: mechanism insight, in situ characterization, performance evaluation, and challenges Nitrate electroreduction: mechanism insight, in-situ characterization, performance evaluation, and challenges, Chemical Society Reviews 50(12) (2021) 6720–6733.

[14] J. Theerthagiri, J. Park, H.T. Das, N. Rahamathulla, E.S.F. Cardoso, A.P. Murthy, G. Maia, D.V.N. Vo, M.Y. Choi, Electrocatalytic conversion of nitrate waste into ammonia: a review, Environmental Chemistry Letters 20(5) (2022) 2929–2949.

[15] S. Garcia-Segura, M. Lanzarini-Lopes, K. Hristovski, P. Westerhoff, Electrocatalytic reduction of nitrate: Fundamentals to full-scale water treatment applications, Applied Catalysis B: Environmental 236 (2018) 546–568.

[16] M. Jiang, Q. Zhu, X. Song, Y. Gu, P. Zhang, C. Li, J. Cui, J. Ma, Z. Tie, Z. Jin, Batch-Scale Synthesis of Nanoparticle-Agminated Three-Dimensional Porous Cu@Cu2O Microspheres for Highly Selective Electrocatalysis of Nitrate to Ammonia, Environmental Science & Technology 56(14) (2022) 10299–10307.

[17] X. Zhao, Y. Jiang, M. Wang, Y. Huan, Q. Cheng, Y. He, T. Qian, C. Yan, Comprehensive understanding of the thriving electrocatalytic nitrate/nitrite reduction to ammonia under ambient conditions, Journal of Energy Chemistry 92 (2024) 459–483.

[18] M.C.P.M. da Cunha, M. Weber, F.C. Nart, On the adsorption and reduction of NO3− ions at Au and Pt electrodes studied by in situ FTIR spectroscopy, Journal of Electroanalytical Chemistry 414(2) (1996) 163–170.

[19] I. Katsounaros, G. Kyriacou, Influence of nitrate concentration on its electrochemical reduction on tin cathode: Identification of reaction intermediates, Electrochimica Acta 53(17) (2008) 5477–5484.

[20] J. Zheng, T. Lu, T.M. Cotton, G. Chumanov, Photoinduced Electrochemical Reduction of Nitrite at an Electrochemically Roughened Silver Surface, The Journal of Physical Chemistry B 103(31) (1999) 6567–6572.

[21] J. Yang, M. Duca, K.J.P. Schouten, M.T.M. Koper, Formation of volatile products during nitrate reduction on a Sn-modified Pt electrode in acid solution, Journal of Electroanalytical Chemistry 662(1) (2011) 87–92.

[22] M. Duca, M.O. Cucarella, P. Rodriguez, M.T.M. Koper, Direct Reduction of Nitrite to N2 on a Pt(100) Electrode in Alkaline Media, Journal of the American Chemical Society 132(51) (2010) 18042–18044.

[23] D.A. Nguyen, M.A. Iwaniw, H.S. Fogler, Kinetics and mechanism of the reaction between ammonium and nitrite ions: experimental and theoretical studies, Chemical Engineering Science 58(19) (2003) 4351–4362.

[24] M.D. Bartberger, W. Liu, E. Ford, K.M. Miranda, C. Switzer, J.M. Fukuto, P.J. Farmer, D.A. Wink, K.N. Houk, The reduction potential of nitric oxide (NO) and its importance to NO biochemistry, Proceedings of the National Academy of Sciences 99(17) (2002) 10958–10963.

[25] H. Niu, Z. Zhang, X. Wang, X. Wan, C. Shao, Y. Guo, Theoretical Insights into the Mechanism of Selective Nitrate-to-Ammonia Electroreduction on Single-Atom Catalysts, Advanced Functional Materials 31(11) (2020).

[26] H.-J. Chun, V. Apaja, A. Clayborne, K. Honkala, J. Greeley, Atomistic Insights into Nitrogen-Cycle Electrochemistry: A Combined DFT and Kinetic Monte Carlo Analysis of NO Electrochemical Reduction on Pt(100), ACS Catalysis 7(6) (2017) 3869–3882.

[27] Y. Zeng, C. Priest, G. Wang, G. Wu, Restoring the Nitrogen Cycle by Electrochemical Reduction of Nitrate: Progress and Prospects, Small Methods 4(12) (2020).

[28] A.C.A. de Vooys, G.L. Beltramo, B. van Riet, J.A.R. van Veen, M.T.M. Koper, Mechanisms of electrochemical reduction and oxidation of nitric oxide, Electrochimica Acta 49(8) (2004) 1307–1314.

[29] X. Zhang, X. Liu, Z.-F. Huang, L. Guo, L. Gan, S. Zhang, M. Ajmal, L. Pan, C. Shi, X. Zhang, G. Yang, J.-J. Zou, Tandem Nitrate Electroreduction to Ammonia with Industrial-Level Current Density on Hierarchical Cu Nanowires Shelled with NiCo-Layered Double Hydroxide, ACS Catalysis 13(22) (2023) 14670–14679.

[30] D. Liu, L. Qiao, S. Peng, H. Bai, C. Liu, W.F. Ip, K.H. Lo, H. Liu, K.W. Ng, S. Wang, X. Yang, H. Pan, Recent Advances in Electrocatalysts for Efficient Nitrate Reduction to Ammonia, Advanced Functional Materials 33(43) (2023).

[31] M.R. Gennero de Chialvo, A.C. Chialvo, Kinetics of hydrogen evolution reaction with Frumkin adsorption: re-examination of the Volmer–Heyrovsky and Volmer–Tafel routes, Electrochimica Acta 44(5) (1998) 841–851.

[32] X. Wang, H. Yao, C. Zhang, C. Li, K. Tong, M. Gu, Z. Cao, M. Huang, H. Jiang, Double-Tuned RuCo Dual Metal Single Atoms and Nanoalloy with Synchronously Expedited Volmer/Tafel Kinetics for Effective and Ultrastable Ampere-Level Current Density Hydrogen Production, Advanced Functional Materials 33(40) (2023).

[33] J. Wang, W. Zang, X. Liu, J. Sun, S. Xi, W. Liu, Z. Kou, L. Shen, J. Wang, Switch Volmer-Heyrovsky to Volmer-Tafel Pathway for Efficient Acidic Electrocatalytic Hydrogen Evolution by Correlating Pt Single Atoms with Clusters Switch Volmer-Heyrovsky to Volmer-Tafel Pathway for Efficient Acidic Electrocatalytic Hydrogen Evolution by Correlating Pt Single Atoms with Clusters, Small 20(25) (2024) 2309427.

[34] M. Jiang, A. Tao, Y. Hu, L. Wang, K. Zhang, X. Song, W. Yan, Z. Tie, Z. Jin, Crystalline Modulation Engineering of Ru Nanoclusters for Boosting Ammonia Electrosynthesis from Dinitrogen or Nitrate, ACS Applied Materials & Interfaces 14(15) (2022) 17470–17478.

[35] D. Xu, Y. Li, L. Yin, Y. Ji, J. Niu, Y. Yu, Electrochemical removal of nitrate in industrial wastewater, Frontiers of Environmental Science & Engineering 12(1) (2018) 9.

[36] Z. Gong, W. Zhong, Z. He, Q. Liu, H. Chen, D. Zhou, N. Zhang, X. Kang, Y. Chen, Regulating surface oxygen species on copper (I) oxides via plasma treatment for effective reduction of nitrate to ammonia, Applied Catalysis B: Environmental 305 (2022) 121021.

[37] F. Lv, M. Sun, Y. Hu, J. Xu, W. Huang, N. Han, B. Huang, Y. Li, F. Lv, Near-unity electrochemical conversion of nitrate to ammonia on crystalline nickel porphyrin-based covalent organic frameworks, Energy & Environmental Science 16(1) (2023) 201–209.

[38] Y. Lv, S.W. Ke, Y. Gu, B. Tian, L. Tang, P. Ran, Y. Zhao, J. Ma, J.L. Zuo, M. Ding, Highly Efficient Electrochemical Nitrate Reduction to Ammonia in Strong Acid Conditions with Fe2M-Trinuclear-Cluster Metal–Organic Frameworks, Angewandte Chemie International Edition 62(27) (2023).

[39] R. Zhang, C. Li, H. Cui, Y. Wang, S. Zhang, P. Li, Y. Hou, Y. Guo, G. Liang, Z. Huang, C. Peng, C. Zhi, Electrochemical nitrate reduction in acid enables high-efficiency ammonia synthesis and high-voltage pollutes-based fuel cells, Nature Communications 14(1) (2023).

[40] H. Shin, S. Jung, S. Bae, W. Lee, H. Kim, Nitrite Reduction Mechanism on a Pd Surface, Environmental Science & Technology 48(21) (2014) 12768–12774.

[41] K. Fan, W. Xie, J. Li, Y. Sun, P. Xu, Y. Tang, Z. Li, M. Shao, Active hydrogen boosts electrochemical nitrate reduction to ammonia, Nature Communications 13(1) (2022).

[42] W. Yang, Z. Chang, X. Yu, R. Shen, L. Wang, X. Cui, J. Shi, Triple Regulations via Fe Redox Boosting Nitrate Reduction to Ammonia at Industrial Current Densities, Angewandte Chemie International Edition 64(3) (2025) e202415300.

[43] J. Li, G. Zhan, J. Yang, F. Quan, C. Mao, Y. Liu, B. Wang, F. Lei, L. Li, A.W.M. Chan, L. Xu, Y. Shi, Y. Du, W. Hao, P.K. Wong, J. Wang, S.-X. Dou, L. Zhang, J.C. Yu, Efficient Ammonia Electrosynthesis from Nitrate on Strained Ruthenium Nanoclusters, Journal of the American Chemical Society 142(15) (2020) 7036–7046.

[44] M.T. de Groot, M.T.M. Koper, The influence of nitrate concentration and acidity on the electrocatalytic reduction of nitrate on platinum, Journal of Electroanalytical Chemistry 562(1) (2004) 81–94.

[45] R. Lange, E. Maisonhaute, R. Robin, V. Vivier, On the kinetics of the nitrate reduction in concentrated nitric acid, Electrochemistry Communications 29 (2013) 25–28.

[46] M. Dortsiou, G. Kyriacou, Electrochemical reduction of nitrate on bismuth cathodes, Journal of Electroanalytical Chemistry 630(1-2) (2009) 69–74.

[47] Y. Chen, C. Chen, W.-H. Huang, C.-W. Pao, C.-C. Chang, T. Mao, J. Wang, H. Fu, F. Lai, N. Zhang, T. Liu, Charge Redistribution in High-Entropy Perovskite Oxide Porous Nanotubes Boosts Nitrate Electroreduction to Ammonia, ACS Nano 18(31) (2024) 20530–20540.

[48] J. Lv, X. Sun, F. Wang, R. Yang, T. Zhang, T. Liang, W. Rong, Q. Yang, W. Xue, L. Wang, X. Xu, Y. Liu, Engineering Nickel Dopants in Atomically Thin Molybdenum Disulfide for Highly Efficient Nitrate Reduction to Ammonia, Advanced Functional Materials 34(49) (2024).

[49] S. Lu, G. Lin, H. Yan, Y. Li, T. Qi, Y. Li, S. Liang, L. Jiang, In Situ Facet Transformation Engineering over Co3O4 for Highly Efficient Electroreduction of Nitrate to Ammonia, ACS Catalysis 14(19) (2024) 14887–14894.

[50] Y. Liu, X. Zhao, C. Long, X. Wang, B. Deng, K. Li, Y. Sun, F. Dong, In situ constructed dynamic Cu/Ce(OH) interface for nitrate reduction to ammonia with high activity, selectivity and stability, Chinese Journal of Catalysis 52 (2023) 196–206.

[51] Z. Zhang, X. Feng, Z. Zhang, L. Chen, W. Liu, L. Tong, X. Gao, J. Zhang, Graphdiyne Enabled Nitrogen Vacancy Formation in Copper Nitride for Efficient Ammonia Synthesis, Journal of the American Chemical Society 146(21) (2024) 14898–14904.